EUROPEAN ORGANIZATION FOR NUCLEAR RESEARCH

CERN/PPE 94-28
9 February 1994

Observation of a narrow scalar meson at 1450 MeV in the reaction $pp \to p_f(\pi^+\pi^-\pi^+\pi^-)p_s$ at 450 GeV/c using the CERN Omega Spectrometer

The WA91 Collaboration

S. Abatzis[1], F. Antinori[4], D. Barberis[4], R.P. Barnes[3], A. Bayes[3], W. Beusch[4], J.N. Carney[3], S. Clewer[3], J.P. Davies[3], D. Di Bari[2], C.J. Dodenhoff[3], D. Evans[4], R. Fini[2], B.R. French[4], B. Ghidini[2], M. Girone[2], A. Jacholkowski[2], J.B. Kinson[3], A. Kirk[4], Y. Kulchitsky[5], V. Lenti[2], R.A. Loconsole[2], S. Maljukov[5], V. Manzari[2], I. Minashvili[5], F. Navach[2], K. Norman[3], E. Quercigh[4], V. Romanovsky[5], N. Russakovich[5], A. Semenov[5], M. Sené[4], R. Sené[4], A. Solovjev[5], G. Tchlatchidze[5], G. Vassiliadis[1], I. Vichou[1], O. Villalobos Baillie[3], M.F. Votruba[3]

1 Athens University, Nuclear Physics Department, Athens, Greece.
2 Dipartimento di Fisica dell'Università and Sezione INFN, Bari, Italy.
3 University of Birmingham, Physics Department, Birmingham, U.K.
4 CERN, European Organization for Nuclear Research, Geneva, Switzerland.
5 JINR, Dubna, Russia.

Abstract

The reaction $pp \to p_f(\pi^+\pi^-\pi^+\pi^-)p_s$ has been studied at 450 GeV/c in an experiment designed to search for gluonic states. In addition to the well known $f_1(1285)$, the $\pi^+\pi^-\pi^+\pi^-$ mass spectrum shows evidence for two states previously only observed by the WA76 experiment, the X(1450) and X(1900). An analysis of the X(1450) shows that it is a relatively narrow state ($\Gamma = 56 \pm 12$ MeV) with $I(J^{PC}) = 0(0^{++})$ which decays to $\rho^0\pi^+\pi^-$. The X(1900) could either be a single broad state ($\Gamma = 370 \pm 70$ MeV) with $I(J^{PC}) = 0(2^{++})$ or possibly two separate states.

Submitted to Physics Letters B

The WA76 collaboration reported the observation of two previously unobserved mesons, which it called the X(1450) and X(1900), decaying to $\pi^+\pi^-\pi^+\pi^-$ in the reaction

$$pp \rightarrow p_f(\pi^+\pi^-\pi^+\pi^-)p_s \tag{1}$$

at 300 GeV/c [1], where the subscripts f and s indicate the fastest and slowest particles in the laboratory respectively. In contrast, no clear evidence was seen for the X(1450) or X(1900) in the 85 GeV/c data of the same experiment. The increase in cross section with increased incident energy [1] is consistent with the formation of these states via a double Pomeron exchange mechanism, which is predicted to be a source of gluonic states [2]. It is interesting to note that the X(1450) state has not been observed in any other production mechanism. One of the main aims of the WA91 experiment [3], which is a continuation of the WA76 experiment, is to confirm the existence of these states and to determine their quantum numbers.

This paper studies the centrally produced exclusive final states formed in reaction (1) at 450 GeV/c. The data come from experiment WA91 which has been performed using the CERN Omega Spectrometer. Details of the layout of the apparatus, the trigger conditions and the data processing have been given in a previous publication [3].

Reaction (1) has been isolated from the sample of events having six outgoing tracks by first imposing the following cuts on the components of the missing momentum: $|missingP_x| < 14.0$ GeV/c, $|missingP_y| < 0.16$ GeV/c and $|missingP_z| < 0.08$ GeV/c, where the x axis is along the beam direction. A correlation between pulse-height and momentum obtained from a system of scintillation counters was used to ensure that the slow particle was a proton.

The quantity Δ defined as

$$\Delta = MM^2(p_f p_s) - M^2(\pi^+\pi^-\pi^+\pi^-) \tag{2}$$

was then calculated for each event and a cut of $|\Delta| \leq 3.0$ (GeV)^2 was used to select the $\pi^+\pi^-\pi^+\pi^-$ channel. Events containing a fast $\Delta^{++}(1232)$ were removed if $M(p_f\pi^+) <$ 1.3 GeV, which left 98860 centrally produced events.

Fig. 1a shows the $\pi^+\pi^-\pi^+\pi^-$ effective mass spectrum. In order to describe the $\pi^+\pi^-\pi^+\pi^-$ mass spectrum it has been fitted, as in WA76 [1], using three Breit-Wigners representing the $f_1(1285)$, the X(1450) and X(1900) plus a background of the form $a(m - m_{th})^b exp(-cm - dm^2)$, where m is the $\pi^+\pi^-\pi^+\pi^-$ mass, m_{th} is the $\pi^+\pi^-\pi^+\pi^-$ threshold mass and a, b, c, d are fit parameters. Reflections from the $\eta\pi^+\pi^-$ decay of the η' and $f_1(1285)$ give small enhancements in the $\pi^+\pi^-\pi^+\pi^-$ mass spectrum in the 0.8 and 1.1 GeV regions due to a slow π^0 from the decay of an η falling within the missing momentum cuts. In order to get a correct description of the $\pi^+\pi^-\pi^+\pi^-$ mass spectrum two histograms representing a Monte Carlo simulation of each reflection have been included in the fit.

Fig. 1b shows the $\pi^+\pi^-\pi^+\pi^-$ effective mass spectrum when no γs are detected in the gamma calorimeter. The η' and $f_1(1285)$ reflections are reduced but the $f_1(1285)$,

X(1450) and X(1900) signals are enhanced relative to the background, indicating that they are not themselves reflections from a channel involving a π^0 which falls within the missing momentum cuts.

The masses and widths determined from the fit [1] are given in table 1. These parameters are consistent with those obtained from the WA76 experiment [1].

Fig. 2a shows the $\pi^+\pi^-\pi^+\pi^-$ mass spectrum when a cut of $|t| \leq 0.15$ GeV^2 has been placed on the four momentum transfer squared at both the fast and slow vertices. The spectrum is fitted using three Breit-Wigners, with masses and widths fixed to the values given in table 1, and a background as described above. Fig. 2b shows the $\pi^+\pi^-\pi^+\pi^-$ mass spectrum when both the slow and fast vertices have $|t| > 0.15$ GeV^2. It appears that the X(1450) and X(1900) are both produced predominantly at low $|t|$.

In order to determine the different reactions that contribute to the observed final states a channel likelihood fit [4] using a modified version of CHAFIT [5] has been used. The program performs a maximum likelihood fit of different incoherent amplitudes and has been used as described in ref. [6]. The main results can be summarised as follows :

1. The $f_1(1285)$ and X(1450) decay dominantly to $\rho^0\pi^+\pi^-$.
2. The X(1900) is found to decay almost equally to $f_2(1270)\pi^+\pi^-$ and $a_2(1320)\pi$.

A spin-parity analysis of the $\pi^+\pi^-\pi^+\pi^-$ channel has been performed using an isobar model. Assuming that only angular momenta up to 2 contribute, the intermediate states considered are $\rho^0\rho^0$, $\rho^0(\pi^+\pi^-)_{Swave}$, $\rho^0(\pi^+\pi^-)_{Pwave}$, $\rho^0(\pi^+\pi^-)_{Dwave}$, $a_1(1260)\pi$, $a_2(1320)\pi$, $f_2(1270)(\pi^+\pi^-)_{Swave}$, $f_2(1270)(\pi^+\pi^-)_{Pwave}$ and $f_2(1270)(\pi^+\pi^-)_{Dwave}$.

The G-parity of the $\pi^+\pi^-$ system is given by $(-1)^{I+L}$ where I is the isospin of the $\pi^+\pi^-$ system and L is the angular momentum between the π^+ and the π^-. Since the G-parity of the $\pi^+\pi^-$ system is positive if the angular momentum, L, is odd then the isospin must be odd. Therefore, assuming the isospin of the decaying resonance to be either 0 or 1 then, in the case of the $\rho^0(\pi^+\pi^-)$ intermediate state, if $L = 1$, then $I = 1$ and the overall isospin of the resonance must be 0. Similarly for the $f_2(1270)(\pi^+\pi^-)$ intermediate state if $L = 0, 2$ then $I = 0$ and the isospin of the decaying resonance must be 0. Therefore a spin analysis can give information not only on the spin of the decaying resonance but also on its isospin by studying the angular momentum of the $\pi^+\pi^-$ pair recoiling against either the ρ^0 or $f_2(1270)$.

The amplitudes have been calculated in the spin-orbit (LS) scheme using spherical harmonics (see the appendix) and are similar to those used in ref. [7]. In order to obtain information about the quantum numbers of the observed peaks a probability weight is constructed for each event i and spin model j:

$$P_j(i) = \frac{|M_j(i)|^2}{\epsilon_j(m_{4\pi}) < |M_j(m_{4\pi})|^2 >} \tag{3}$$

[1] In order to calculate the errors on the fit parameters many different mass distributions have been generated from the original by varying the number of events in each bin according to a Poisson distribution. These spectra have then been refitted and the variation in values obtained from these fits has been used to calculate the errors quoted.

where M_j represents a choice of one of the $A^{(L,S)}(J, J_z)$ terms given in the appendix and ϵ_j denotes the acceptance for model j at the $\pi^+\pi^-\pi^+\pi^-$ mass $m_{4\pi}$. This quantity compares the matrix element squared of the observed event with the Monte Carlo expectation of the model at the $\pi^+\pi^-\pi^+\pi^-$ mass, integrated over the phase space variables.

For each model j a histogram of the $\pi^+\pi^-\pi^+\pi^-$ mass spectrum is filled with each event weighted by $P_j(i)$. This allows a visual determination of the dominant waves since the resonance peaks should appear predominantly in the histogram corresponding to its spin quantum numbers. The four histograms which show the most resonant activity are shown in figure 3. Fig 3a shows the effect of weighting using the $J^P = 1^+\rho(\pi\pi)_{Pwave}$ which clearly picks out the $J^P = 1^+$ $f_1(1285)$ giving confidence in the method [2]. The X(1450) is clearly seen in the $J^P = 0^+\rho(\pi\pi)_{Pwave}$ distribution (fig. 3b) and the X(1900) is seen in the $J^P = 2^+a_2(1320)\pi$ and $J^P = 2^+f_2(1270)(\pi\pi)_{Swave}$ distributions (figs. 3c and d respectively). No peaks are observed in the $\rho(\pi\pi)_{Swave}$ or $\rho(\pi\pi)_{Dwave}$ distributions, showing that the peaks observed have $I = 0$.

In order to perform a spin parity analysis the negative log likelihood function, $\mathcal{L}_j = -\sum_i \log P_j(i)$, is defined by combining the probabilities of all events in 40 MeV $\pi^+\pi^-\pi^+\pi^-$ mass bins from 1.02 to 2.82 GeV. In order to include more than one model in the fit the incoherent sum of various event fractions a_j is calculated:

$$\mathcal{L} = -\sum_i \log\left(\sum_j a_j P_j(i) + (1 - \sum_j a_j)\right) \tag{4}$$

where the term $(1 - \sum_j a_j)$ represents the phase space background. The function $\mathcal{L}$ is then minimised using MINUIT [8]. Coherence between different J^P states and between different isobar amplitudes of a given J^P have been neglected in the fit. Different combinations of waves and isobars have been tried and insignificant contributions have been removed from the final fit. The results of the best fit are shown in fig 4. Superimposed on the figures are the resonance contributions coming from a fit to the mass spectrum in 40 MeV bins. As can be seen from fig. 4a the $J^P = 1^+$ $\rho(\pi\pi)_{Pwave}$ clearly describes the $f_1(1285)$ in size and shape. Fig. 4b shows the $J^P = 0^+\rho(\pi\pi)_{Pwave}$ distribution where in addition to the X(1450) peak there is a broad enhancement. Figs. 4c and d show that neither the $J^P = 2^+a_2(1320)\pi$ nor the $J^P = 2^+f_2(1270)(\pi\pi)_{Swave}$ alone can describe the X(1900). However, the sum of the two (fig. 4e) represents the X(1900) quite well. This could indicate that the peak at 1900 MeV is composed of two states with the same spin parity.

In order to give a measure of the significance of the quantum number determination for the X(1450) the change in log likelihood in the two 40 MeV bins around the X(1450) has been calculated by replacing the $J^P = 0^+\rho(\pi\pi)_{Pwave}$ amplitude with other amplitudes of different spin parities. The results are summarised in table 2. The next best fit is for the $J^P = 2^+\rho(\pi\pi)_{Pwave}$ amplitude which yields a likelihood difference of $\Delta\mathcal{L} = 252$ worse than the $J^P = 0^+$ assignment, corresponding to $n = \sqrt{2\Delta\mathcal{L}} = 22.5$ standard deviations [9].

[2] In the analysis of the $f_1(1285)$ and X(1450) there is little difference in the result if the $\rho\rho$ amplitude is used instead of the $\rho(\pi\pi)_{Pwave}$.

Using Monte Carlo simulations it has been found that the feed through from one spin parity to another is negligible and that the peaks in the spin analysis can not be produced by phase space or acceptance effects.

The spin analysis performed by the WA76 collaboration in reference [1] gave an ambiguity between the $J^P = 2^+$ and 1^- waves. An error in the construction of the 0^+ amplitude meant that this wave was not considered. If this error is corrected then the result of the WA76 analysis is that the $J^P = 0^+, 1^-$ and 2^+ waves are ambiguous. However the method employed there only fitted two angles and it fitted these separately. The method used in this paper is able to resolve the ambiguity since it fits six angles and the intermediate resonance masses simultaneously. If the method presented in this paper is applied to the WA76 data it also shows that the spin of the X(1450) is 0^+.

In conclusion, the analysis of the centrally produced $\pi^+\pi^-\pi^+\pi^-$ channel presented in this paper confirms the existence of the X(1450) and X(1900) observed by the WA76 experiment. The X(1900) could either be a single broad state which decays to $a_2(1320)\pi$ and $f_2(1270)\pi\pi$ and has $J^{PC} = 2^{++}$ or possibly two separate states each having $J^{PC} = 2^{++}$. The X(1450) is a narrow state with $I(J^{PC}) = 0(0^{++})$ and is a very interesting state since it is only observed in central production, which is believed to be gluon rich, and it does not easily fit into the standard ground state $q\overline{q}$ nonet which is already overfull.

Acknowledgements

We would like to thank M. Feindt for his helpful suggestions and comments on the spin analysis presented in this paper.

Appendix

In this appendix the spin amplitudes for a $\rho\pi\pi$ final state are described in the spin-orbit (LS) coupling scheme. The square of the amplitudes calculated in the following gives the weight which $\rho\pi\pi$ phase space events need in order to describe a process with a specific J^P, helicity and subresonance (isobar). The two distinct processes considered are the $\rho\rho$ and $a_j\pi$ final states, where $j = 1, 2$. The construction of the other amplitudes will be discussed after these examples.

Firstly for the $\rho\rho$ amplitudes. Both spin-1 particles are first coupled to a total spin denoted by the spin function:

$$f_S(S, s_z) = \sum_{m_{\rho_1}, m_{\rho_2}} \left(\begin{array}{cc|c} 1 & 1 & S \\ m_{\rho_1} & m_{\rho_2} & s_z \end{array} \right) \times Y_1^{m_{\rho_1}}(cos\theta_{\pi_1^+}, \phi_{\pi_1^+}) Y_1^{m_{\rho_2}}(cos\theta_{\pi_2^+}, \phi_{\pi_2^+}) \quad (5)$$

The angles involved measure the directions of each π^+ in their respective ρ CMS system, defined by transforming from the overall centre of mass into the centre of mass of the exchanged particles and from there into the ρ centre of mass. All angles are with respect to the exchanged particle axis. The expression in brackets denotes a standard Clebsch-Gordan coefficient which is non-zero only for $m_{\rho_1} + m_{\rho_2} = s_z$. In the second step the spin functions are coupled with the orbital angular momentum functions to give the total spin function:

$$A^{(L,S)}(J, J_z) = \sum_{m_L, s_z} \left(\begin{array}{cc|c} L & S & J \\ m_L & s_z & J_z \end{array} \right) \times Y_L^{m_L}(cos\theta_\rho, \phi_\rho) f_S(S, s_z) \times BW(\rho_1) BW(\rho_2) \quad (6)$$

The angles appearing here describe the ρ in the exchanged particle centre of mass. A relativistic Breit-Wigner amplitude is used for the description of the propagation of the ρs.

In order to describe the $\rho(\pi\pi)_{Xwave}$ decay, where $X = S$, P or D, equation (5) becomes

$$f_S(S, s_z) = \sum_{m_{\rho_1}, m_{\pi\pi}} \left(\begin{array}{cc|c} 1 & X & S \\ m_{\rho_1} & m_{\pi\pi} & s_z \end{array} \right) \times Y_1^{m_{\rho_1}}(cos\theta_{\pi_1^+}, \phi_{\pi_1^+}) Y_X^{m_{\pi\pi}}(cos\theta_{\pi_2^+}, \phi_{\pi_2^+}) \quad (7)$$

and $BW(\rho_2)$ is removed from equation (6). For the $f_2(1270)\pi\pi$ decay equation (5) becomes

$$f_S(S, s_z) = \sum_{m_{f_2}, m_{\pi\pi}} \left(\begin{array}{cc|c} 2 & X & S \\ m_{f_2} & m_{\pi\pi} & s_z \end{array} \right) \times Y_1^{m_{f_2}}(cos\theta_{\pi_1^+}, \phi_{\pi_1^+}) Y_X^{m_{\pi\pi}}(cos\theta_{\pi_2^+}, \phi_{\pi_2^+}) \quad (8)$$

and in equation (6) $BW(\rho_1)$ becomes $BW(f_2(1270))$ and $BW(\rho_2)$ is removed.

Secondly for the $a_j\pi$ final state. To begin with, the ρ and the π are combined to give the spin function for the a_j intermediate state:

$$f_a(S, s_z) = \sum_{m_l, m_\rho} \left(\begin{array}{cc|c} l & 1 & S \\ m_l & m_\rho & s_z \end{array} \right) \times Y_l^{m_l}(cos\theta_\rho, \phi_\rho) Y_1^{s_z}(cos\theta_\pi, \phi_\pi) \quad (9)$$

where θ_ρ is measured in the a_j rest frame. For an $a_1(1260)$ intermediate state $l = 0$ and for an $a_2(1320)$ intermediate state $l = 2$.

The a_j intermediate state is then coupled with the other π to produce the total spin state:

$$A^{(L)}(J, J_z) = \sum_{m_L, s_z} \left(\begin{array}{cc|c} L & S & J \\ m_L & s_z & J_z \end{array} \right) \times Y_L^{m_L}(cos\theta_a, \phi_a) f_a(S, s_z) BW(a_j) \qquad (10)$$

Since both positive and negative helicity amplitudes should be produced at equal rates, the mean of both squared helicity amplitudes is used in the fit.

References

[1] T. A. Armstrong *et al.,* Phys. Lett. **B228** (1989) 536.

[2] D. Robson *et al.,* Nucl. Phys. **B130** (1977) 328.

[3] F. Antinori *et al.,* CERN/PPE 93-133 (To be published in Il Nuovo Cimento).

[4] P.E.Condon and P.Cowell, Phys. Rev. **D9** (1974) 2268.

[5] Ph.Gavillet and J.C.Marin, CHAFIT, CERN/D.Ph.II/PROG 75-2,1975.

[6] T. A. Armstrong *et al.,* Zeit. Phys. **C43** (1989) 55.

[7] H. J. Behrend *et al.,* Phys. Lett. **B257** (1991) 505.

[8] F. James and M. Roos, MINUIT Computer Physics Communications **10** (1975) 343; CERN-D506 (1989).

[9] K. McDonald *Properties of the maximum likelihood method* CALT-68-321.

Tables

Table 1: Parameters of resonances in the fit to the $\pi^+\pi^-\pi^+\pi^-$ mass spectrum

	Mass (MeV)	Width (MeV)	Observed decay mode	$I(J^{PC})$
$f_1(1285)$	1280 ± 2	40 ± 5	$\rho\pi\pi$	$0(1^{++})$
X(1450)	1446 ± 5	56 ± 12	$\rho\pi\pi$	$0(0^{++})$
X(1900)	1926 ± 12	370 ± 70	$a_2(1320)\pi$ $f_2(1270)\pi\pi$	$0(2^{++})$

Table 2: Likelihood difference between $J^P = 0^+$ and other J^P states decaying to $\rho(\pi\pi)_{Pwave}$ for the X(1450) region.

J^P	0^-	1^-	1^+	2^-	2^+
$\Delta\mathcal{L}$	4633	3668	4715	3907	252

Figures

Figure 1: The $\pi^+\pi^-\pi^+\pi^-$ effective mass spectrum with fit using 3 Breit-Wigners: a) total spectrum and b) requiring no γs detected in the gamma calorimeter.

Figure 2: The $\pi^+\pi^-\pi^+\pi^-$ effective mass spectrum for a) $|t(slow)| \leq 0.15$ (GeV)^2 and $|t(fast)| \leq 0.15$ (GeV)^2 with fit using 3 Breit-Wigners and b) $|t(slow)| > 0.15$ (GeV)^2 and $|t(fast)| > 0.15$ (GeV)^2 with fit using a single Breit-Wigner to describe the $f_1(1285)$.

Figure 3: The $\pi^+\pi^-\pi^+\pi^-$ effective mass spectrum weighted by: a) 1^+ $\rho(\pi\pi)_{Pwave}$, b) 0^+ $\rho(\pi\pi)_{Pwave}$, c) 2^+ $a_2(1320)\pi$ and d) 2^+ $f_2(1270)\pi\pi$.

Figure 4: Results of the spin parity analysis: a) 1^+ $\rho(\pi\pi)_{Pwave}$, b) 0^+ $\rho(\pi\pi)_{Pwave}$, c) 2^+ $a_2(1320)\pi$, d) 2^+ $f_2(1270)(\pi\pi)_{Swave}$ and e) sum of 2^+ $a_2(1320)\pi$ and 2^+ $f_2(1270)(\pi\pi)_{Swave}$. The superimposed curve is the resonance contribution coming from a fit to the mass spectrum.

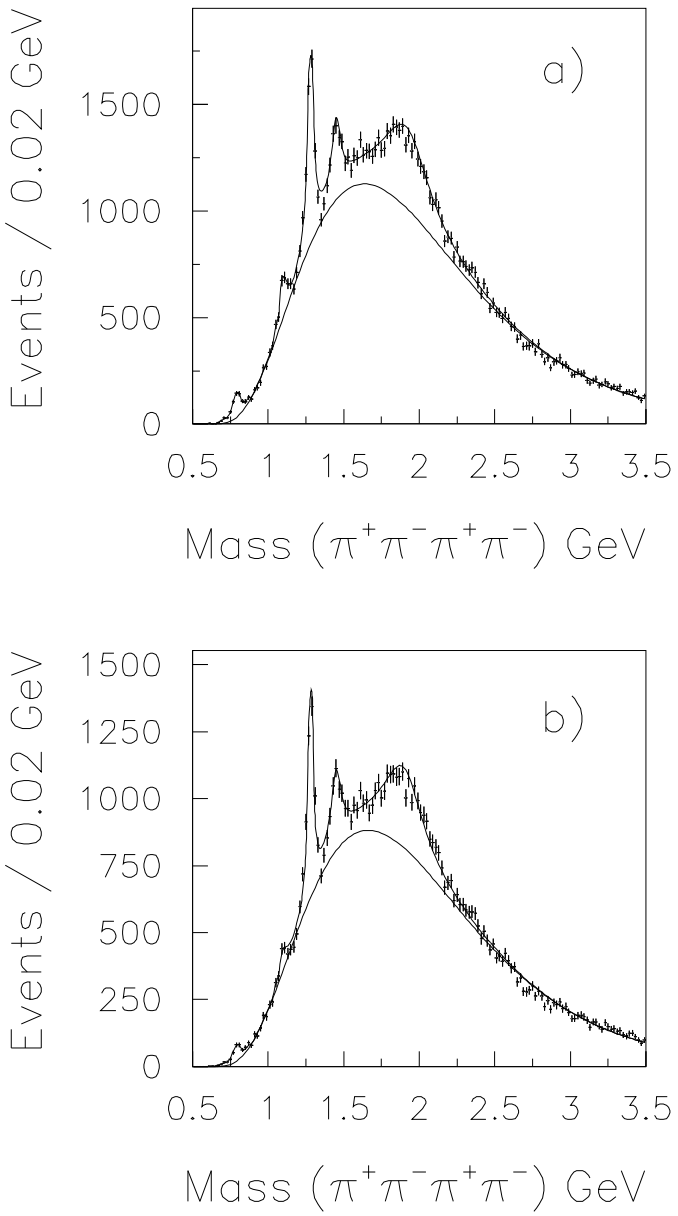
a)
b)
Events / 0.02 GeV
Mass $(\pi^+\pi^-\pi^+\pi^-)$ GeV
0
500
1000
1500
250
750
1250
0.5
1
1.5
2
2.5
3
3.5

Figure 1

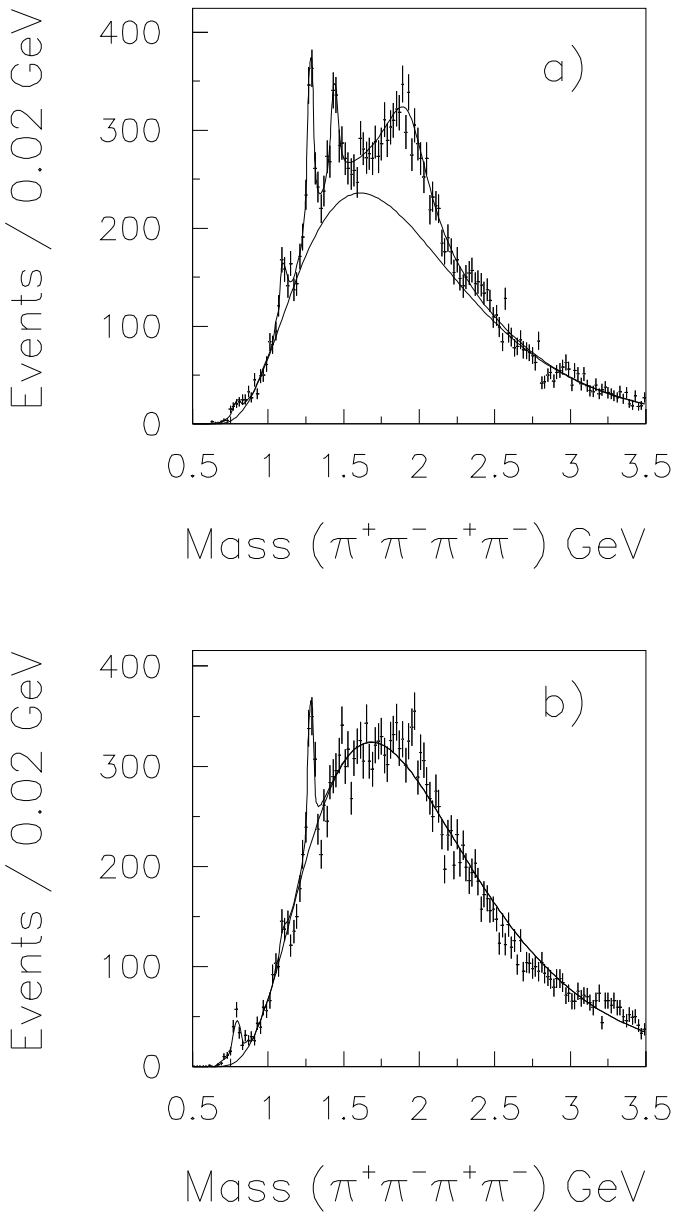
Events / 0.02 GeV
400
300
200
100
0
a)
0.5
1
1.5
2
2.5
3
3.5
Mass $(\pi^+\pi^-\pi^+\pi^-)$ GeV
Events / 0.02 GeV
400
300
200
100
0
b)
0.5
1
1.5
2
2.5
3
3.5
Mass $(\pi^+\pi^-\pi^+\pi^-)$ GeV

Figure 2

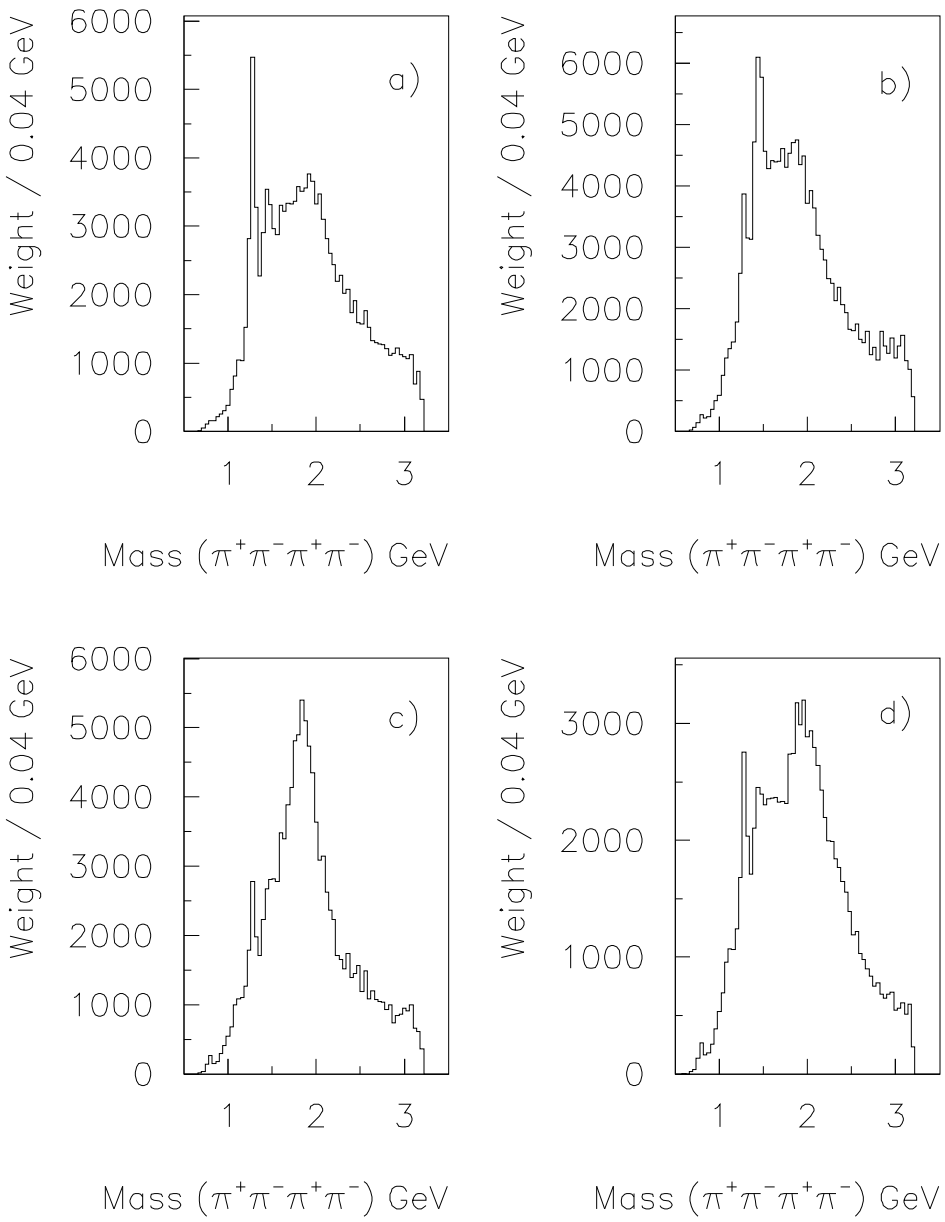
a)
b)
c)
d)
Weight / 0.04 GeV
Mass $(\pi^+\pi^-\pi^+\pi^-)$ GeV
0
1000
2000
3000
4000
5000
6000
1
2
3

Figure 3

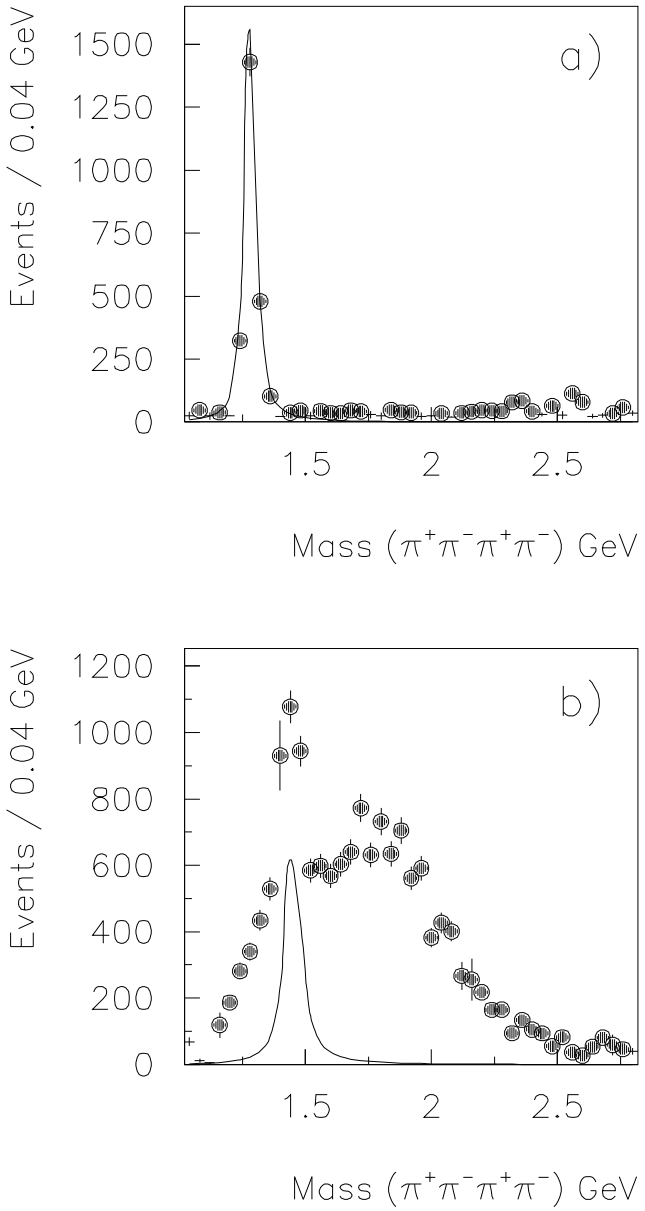
a)
Events / 0.04 GeV
1500
1250
1000
750
500
250
0
1.5
2
2.5
Mass $(\pi^+\pi^-\pi^+\pi^-)$ GeV
b)
Events / 0.04 GeV
1200
1000
800
600
400
200
0
1.5
2
2.5
Mass $(\pi^+\pi^-\pi^+\pi^-)$ GeV

Figure 4

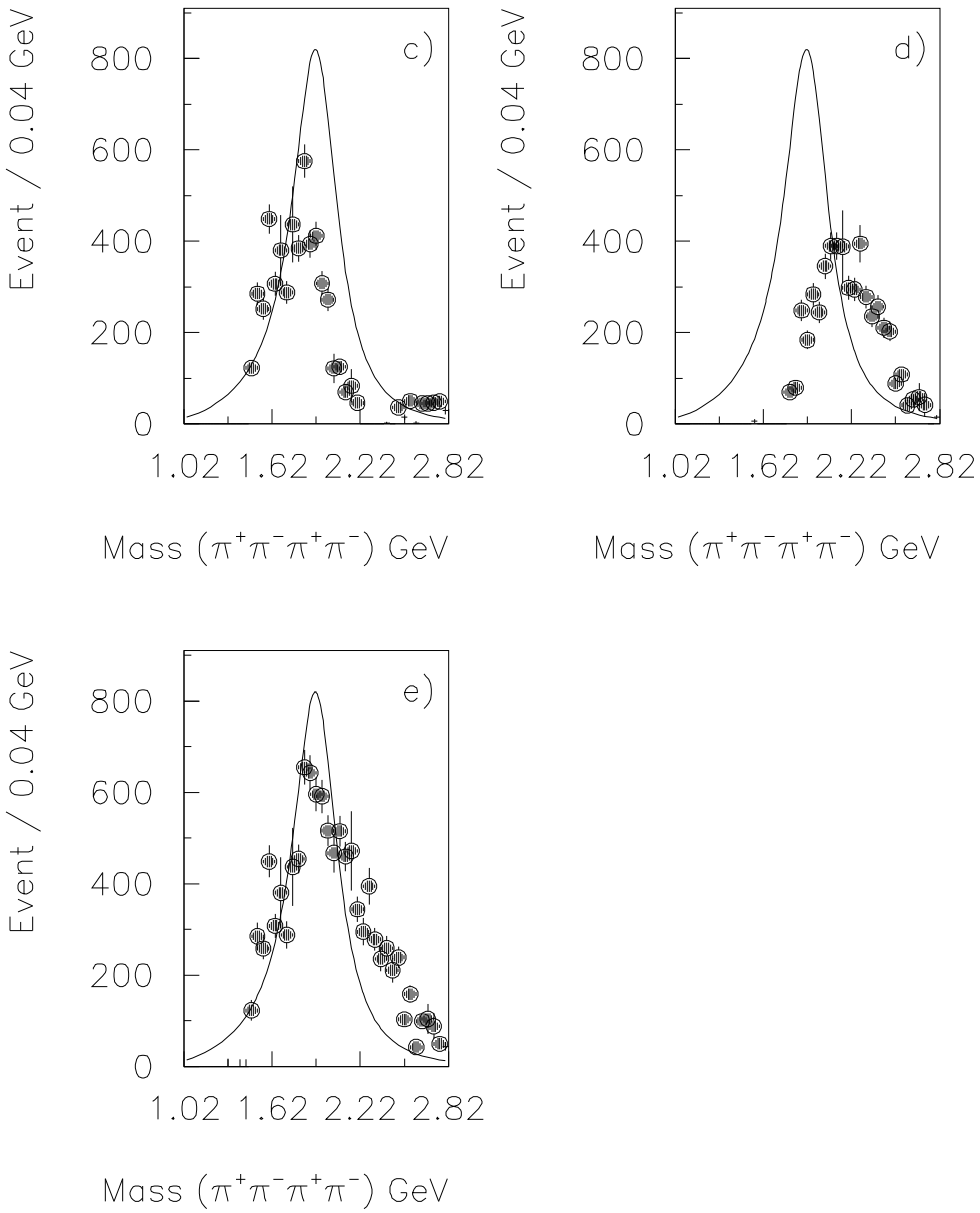
c)
d)
e)
Event / 0.04 GeV
800
600
400
200
0
1.02 1.62 2.22 2.82
Mass ($\pi^+\pi^-\pi^+\pi^-$) GeV

Figure 4